

## Synthesis of Hybrid Monolithic Columns Using a Click Chemistry Reaction for Application in Capillary Liquid Chromatography

Marcella E. P. Schmidt<sup>a</sup> and Carla B. G. Bottoli<sup>✉\*,a</sup>

<sup>a</sup>Instituto de Química, Universidade Estadual de Campinas,  
PO Box 6154, 13084-971 Campinas-SP, Brazil

Hybrid monolithic columns present characteristics of both silica and organic monoliths, such as good mechanical properties, wide pH tolerance, high permeability and stability and little swelling or shrinkage. A common way to prepare this type of material is by using alkoxysilanes and organic monomers via the sol-gel process and click chemistry reactions. In this paper, a co-condensation organic-silica hybrid monolith was prepared based on tetramethoxysilane (TMOS) and vinyltrimethoxysilane (VTMS) as precursors for the sol-gel process. The hybrid monolithic matrix was modified with dodecanethiol through the thiol-ene click chemistry reaction and the resulting material was compared with a dodecanesilane bonded phase column, in order to evaluate the differences in the chromatographic performance of a stationary phase prepared by a classic reaction or by a thiol-ene click reaction. Additionally, the stability of the thiol-ene column over time was evaluated. The effects of different synthetic proportions were investigated in detail by scanning electron microscopy (SEM), scanning capacitively coupled contactless conductivity detection (sC<sup>4</sup>D), Fourier-transform infrared spectroscopy (FTIR) and retention behavior in capillary liquid chromatography (cLC). The hybrid monolithic column prepared with dodecanethiol was the best one for the separation of alkylbenzenes and polycyclic aromatic hydrocarbons by cLC-UV.

**Keywords:** hybrid monolith column, capillary liquid chromatography, thiol-ene click chemistry reactions, sol-gel process

### Introduction

Capillary liquid chromatography (cLC) is based on the same concepts as high-performance liquid chromatography (HPLC), but the inner diameters of the columns (0.1-0.5 mm) are reduced, requiring resizing of the tubings, pumps, injectors and detectors. This reduction results in lower consumption of mobile phase, better column performance and easier interfacing with other techniques, especially mass spectrometry (MS).<sup>1,2</sup> Evolving from HPLC to cLC, there are also advances in the materials used as stationary phases for capillary columns in cLC. The newest stationary phases for capillary columns are more efficient, allow higher flow rates with a minimum of increased pressure, have higher plate numbers and higher permeability, due to less mass transfer, lower pressures and higher porosities.<sup>3-8</sup> There are three types of columns that can be used in cLC: packed columns, open-tubular columns and monolithic columns. Since the beginning of cLC, monolithic columns have

aroused interest in separation science mainly because of their advantages, compared to packed columns.<sup>9,10</sup>

According to Guiochon,<sup>11</sup> a monolith is a continuous block of a porous and permeable material, in which solvent can percolate and has a large enough surface area to exhibit retention of a significant number of analytes. The morphological characteristics of monolithic columns and wide functionalization diversity for specific applications are advantages that indicate that monoliths are an alternative to packed columns.

The monolithic stationary phases can be classified in three categories; inorganic silica-based,<sup>3,9</sup> polymer-based<sup>12</sup> and organic-silica hybrid based.<sup>13</sup> Since 2000, the latter has been attracting much research as an alternative that combines the best characteristics of inorganic and organic columns.

In 2000, Hayes and Malik<sup>13</sup> synthesized the first organic-silica hybrid monolithic column, initiating a new manner to synthesize the monoliths, based on the direct incorporation of organic portions in the silica matrix via the sol-gel process.<sup>14</sup> Such syntheses generate materials with advantages compared to other types of monoliths,

\*e-mail: carlab@unicamp.br

such as good mechanical properties, less shrinkage during the manufacturing process, wide tolerance to pH, high permeability and good column efficiency.<sup>14-18</sup>

The preparation of hybrid monoliths can be carried out by different processes: (a) sol-gel synthesis using tri- and tetra-alkoxysilanes with organic groups as precursors; (b) reactions with organic-inorganic (non-silica) reagents; (c) reactions with organic-silica/metal reagents; (d) free radical polymerization; (e) ring-opening polymerization and (f) one-pot chemistry using: (i) alkoxysilanes with organic monomers and (ii) polyhedral oligomeric silsesquioxanes-based monomers (POSS). This last one can occur in two different solution systems: organic solvent/ aqueous solution and nonaqueous solution.<sup>3,10,12,14,19</sup> There are other approaches to the preparation of hybrid monolithic columns that use ionic liquids and nanoparticles of carbon, gold or silica.<sup>8</sup> In the processes of sol-gel synthesis, groups can be incorporated after synthesis by secondary reactions to achieve specific characteristics. One way to do this is via click chemistry reactions, which result in improved efficiency and selectivity of the materials.<sup>20</sup> The use of click chemistry reactions allows a high conversion under mild conditions, being simple and efficient syntheses. These properties bring a considerable improvement to the synthesis of new stationary phase materials, especially in microsystems, such as monolithic columns. Thus, using these reactions to synthesize capillary monolithic columns could present benefits making click chemistry reactions an interesting way of synthesis to be explored for capillary and nano-LC.

This type of chemical reaction was defined by Sharpless and co-workers<sup>21</sup> in 2001 as “a set of powerful, highly reliable and selective reactions for rapid synthesis of new compounds via heteroatom (C–X–C) bonds”. In the context of separation chemistry, more specifically for the production of monolithic columns, the click-polymerizations reactions can be classified as: (i) azide-alkyne cycloaddition catalyzed by copper(I) (CuAAC); (ii) ring-opening polymerization; (iii) thiol-ene/ino and (iv) thiol-(meth) acrylate.<sup>8,20</sup> Specifically, for the preparation of monolithic columns, these reactions must be non-reactive towards oxygen and occur only within the capillary. Among the types of click chemistry reactions, thiol-ene is the most commonly used today for obtaining monolithic materials.<sup>2,16,20,22-25</sup> Zou and co-workers<sup>16</sup> prepared hybrid monoliths via sol-gel chemistry and the surface was tailored via a thiol-ene click reaction by using 1-octadecanethiol, sodium 3-mercapto-1-propanesulfonate and 2,2-(ethylenedioxy)diethanethiol/vinylphosphonic acid. Also, the preparation of octadecyl-functionalized and strong cation exchange (SCX) monolithic columns has been

investigated for proteomic analysis in CLC-MS/MS and in SCX-reversed phase (RP)LC-MS/MS, respectively.<sup>16</sup>

In this work, we present the preparation of an organic-silica hybrid monolith, prepared using tetramethoxysilane (TMOS) and vinyltrimethoxysilane (VTMS) as precursors for the sol-gel process. Through the thiol-ene click reaction, a new stationary phase was prepared using dodecanethiol to modify the hybrid monolithic matrix in order to increase hydrophobic interactions inside the column. A hypervinylation reaction was also evaluated before the thiol-ene reaction to ensure that all the sites on the monolith surface were replaced by vinyl groups and were suitable for the thiol-ene reaction. We have examined the effects of functional organic moieties comparing dodecanethiol with a dodecanesilane bonded phase tailored on a surface of a hybrid monolith. The stability of the thiol-ene column was evaluated as well as the morphology of the columns using scanning electron microscopy (SEM), scanning capacitively coupled contactless conductivity detection (sC<sup>4</sup>D), Fourier-transform infrared spectroscopy (FTIR) and the retention behavior of test compounds in cLC.

## Experimental

### Chemicals and materials

All the reagents were of analytical grade. Tetramethoxysilane (TMOS), vinyltrimethoxysilane (VTMS), poly(ethylene glycol) (PEG,  $M_n = 10000 \text{ g mol}^{-1}$ ), glacial acetic acid, triethylamine (TEA), dodecanethiol (DDT), 2,2'-azobisisobutyronitrile (AIBN), trichlorododecylsilane (TCDDS) and the standards of alkylbenzenes were obtained from Sigma-Aldrich (Steinheim, Germany). The sodium hydroxide solution was obtained from Agilent Technologies (Walbronn, Germany), vinyltrimethoxysilane (VDMES) was obtained from BeanTown Chemical Inc. (Hudson, MA, USA) and urea was obtained from Riedel-de Haën (Seelze, Germany). Methanol, diethyl ether and acetonitrile, all HPLC grade, were obtained from Tedia (Fairfield, USA). Fused-silica capillaries with 100  $\mu\text{m}$  ID and 360  $\mu\text{m}$  OD were purchased from Agilent Technologies (Walbronn, Germany) and the water used in the experiments was purified by a Milli-Q system from Millipore (Bedford, USA).

### Pretreatment of the capillary

Prior to use, the fused-silica capillary was washed and filled with 1.0 mol L<sup>-1</sup> sodium hydroxide solution, using a KDS-100 syringe pump, KdScientific (Holliston, USA),

sealed with rubber connectors and kept in a vacuum oven model LSDZF-6021 from Logen Scientific (Diadema, Brazil) at 120 °C for 2 h. Next, the capillary was flushed with purified water to neutrality and dried by purging with nitrogen gas for 1 h.

#### Preparation of the monolithic columns

The pre-polymerization mixture was prepared based on that of Liu *et al.*,<sup>16</sup> in which hybrid silica monoliths were first synthesized by a sol-gel synthesis with different amounts of PEG 10, urea, acetic acid, TMOS and VTMS, according to Table 1. The sol-gel solution was stirred at 0 °C for 1 h to obtain a homogeneous solution. This mixture was introduced into the pretreated capillary by a syringe pump and kept at 55 °C for 12 h for gelification and ageing in a vacuum oven. Then, the temperature was raised to 120 °C with a heating ramp of 0.5 °C min<sup>-1</sup> and maintained for 2 h (this is denoted as monolith 1). Some of these columns were flushed with a VDMES/

TEA/MeOH solution and kept at 80 °C for 24 h. This increases the content of vinyl groups in the monolithic matrix (denoted monolith 2). The derivatization of the hybrid monoliths was carried out via the thiol-ene click reaction between the dodecanethiol and the vinyl groups on the surface of the monoliths. A solution in diethyl ether of dodecanethiol/AIBN (10/0.5 wt.%) mixture was used to flush the columns that were then incubated at 70 °C for 12 h. The same process was performed with monoliths 1 and 2, resulting in monoliths 3 and 4, respectively. Scheme 1 describes the synthetic procedures for the preparation of these materials and Table 1 presents the amounts of reagents and their effects on the chromatographic and morphological parameters. All the monolithic capillaries were cooled to ambient temperature and washed with 100% MeOH between each synthetic step and prior to each analysis. Monolith 1 was also derivatized with a trichlorododecylsilane (TCDDS) solution in toluene for 24 h at 100 °C (denoted monolith 5). Three toluene solutions with different contents of TCDDS

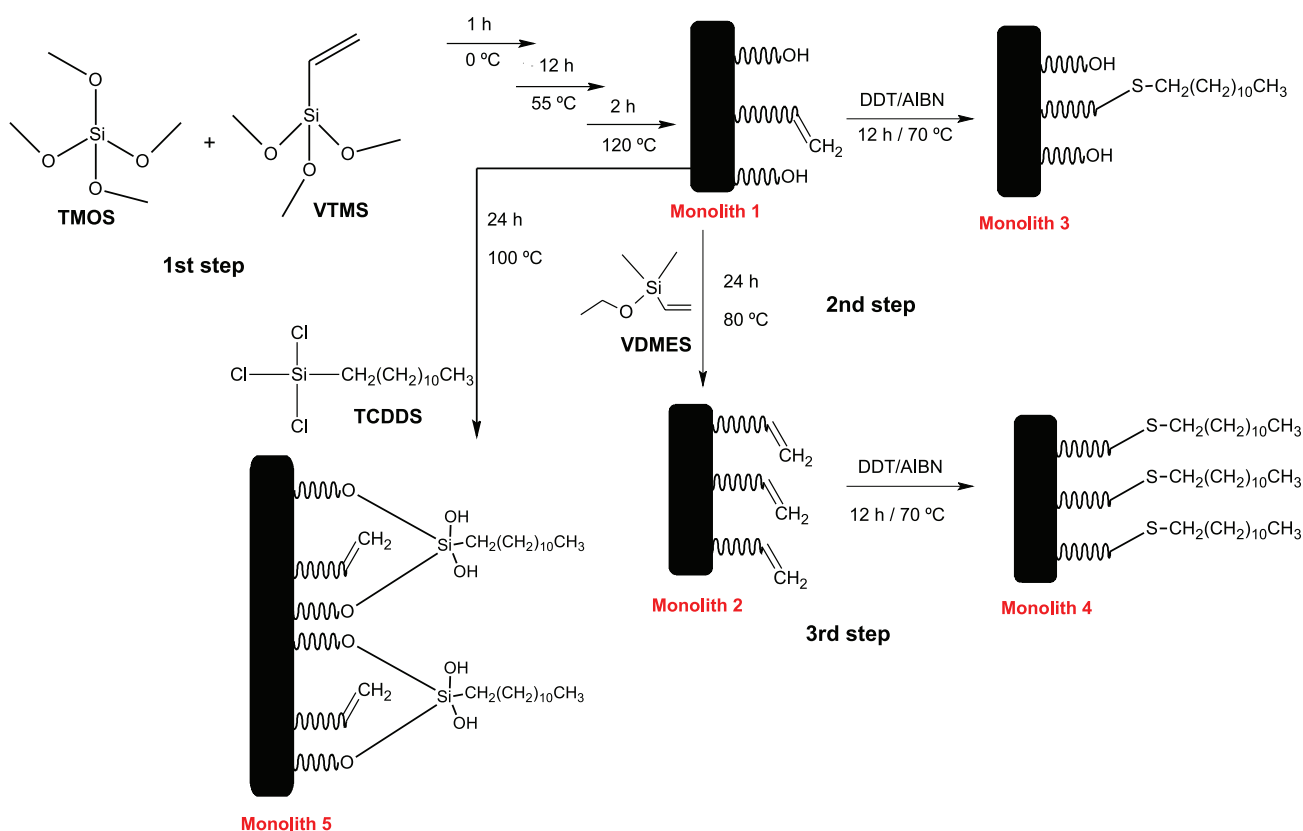
**Table 1.** Effect of synthesis parameters on the formation of vinyl hybrid monoliths

Column	Acetic acid / mL	PEG / mg	Urea / mg	TMOS:VTMS	Optical morphology	Permeability (K) <sup>a</sup> / (× 10 <sup>-14</sup> m <sup>2</sup> )	N <sup>b</sup> / m <sup>-1</sup>	As <sub>10%</sub> <sup>c</sup>	Rs <sup>d</sup>
A	1.8	180	162	3:1	homogeneous and opaque	0.114	11900	0.9	2.0
B	2.2	180	162	3:1	slightly detached	0.117	15900	1.2	3.0
C	1.8	220	162	2.5:1	homogeneous and opaque	0.111	1800	1.0	1.1
D	2.2	220	162	3.6:1	homogeneous and opaque	7.990	10000	1.3	2.2
E	1.8	180	198	3.6:1	seriously detached	– <sup>e</sup>	–	–	–
F	2.2	180	198	2.5:1	seriously detached	– <sup>e</sup>	–	–	–
G	1.8	220	198	3:1	homogeneous and opaque	– <sup>e</sup>	–	–	–
H	2.0	200	180	3:1	homogeneous and opaque	0.127	16500	1.2	3.6
I <sup>f</sup>	2.0	200	180	3:1	homogeneous and transparent	7.470	1400	1.1	1.7
J <sup>g</sup>	2.0	200	180	3:1	homogeneous and transparent	3.760	4300	1.4	2.3
K <sup>h</sup>	2.0	200	180	3:1	homogeneous and transparent	– <sup>e</sup>	–	–	–

<sup>a</sup>K = F × η × L / (ΔP × π × r<sup>2</sup>), where F is the mobile phase flow rate, η is the mobile phase viscosity, ΔP is the pressure drop across the column, L is the column length, and r is the inner radius of the column.<sup>26</sup> Backpressure was obtained with ACN:H<sub>2</sub>O 90:10 (v/v) as mobile phase at 0.7 μL min<sup>-1</sup>; <sup>e</sup>efficiency (plates m<sup>-1</sup>) where N can be calculated based on the formula:  $N = 5.54 \left( \frac{t_R}{w_{50\%}} \right)^2$ , where t<sub>R</sub> is the retention time and w<sub>50%</sub> is the peak width at half-height;

<sup>c</sup>As<sub>10%</sub>: asymmetry for the most retained compound, calculated based on the formula:  $A = \frac{wB_{10\%}}{wA_{10\%}}$ , where wA<sub>10%</sub> is the peak width of the right half side of the peak and wB<sub>10%</sub> is the peak width of the left half side of the peak; <sup>d</sup>resolution factor (Rs) between adjacent peaks 5-6 of alkylbenzene mixtures calculated

based on the formula:  $2 \left( \frac{t_{R_2} - t_{R_1}}{w_{b1} + w_{b2}} \right)$ , where t<sub>R</sub> is the retention time and w<sub>b</sub> is the peak width; <sup>e</sup>too dense to pump through the capillary; <sup>f</sup>the monolith was prepared in the same way as monolith H through the 1<sup>st</sup> step. Then the monolith was reacted with a 30:70 (v/v) TCDDS/toluene solution; <sup>g</sup>the monolith was prepared in the same way as monolith H through the 1<sup>st</sup> step. Then the monolith was reacted with a 50:50 (v/v) TCDDS/toluene solution; <sup>h</sup>the monolith was prepared in the same way as monolith H through the 1<sup>st</sup> step. Then the monolith was reacted with a 70:30 (v/v) TCDDS/toluene solution. PEG: poly(ethylene glycol); TMOS:VTMS: tetramethoxysilane:vinyltrimethoxysilane. PEG: poly(ethylene glycol); TMOS: tetramethoxysilane; VTMS: vinyltrimethoxysilane.



**Scheme 1.** Synthesis route and functionalization of organic-silica hybrid monoliths based on the thiol-ene click reaction.

were used to functionalize the hybrid silica monolith: 30% (column I), 50% (column J) and 70% (column K).

#### Physical characterization

Evaluations of column contents were made by optical microscopy with a Motic BA300 microscope (Diadema, Brazil). The morphological evaluation of the monolithic columns was made by scanning electron microscopy (SEM), using a Jeol JSM-6360 (Tokyo, Japan). The extremities of the capillaries were cut off and cross-sections portions of approximately 5 mm length were fixed with a double-sided carbon tape onto the sample holder. Then, they were covered with an Au/Pd metallization of about 10 nm thickness. The micrographs were obtained with several magnifications, to provide the best visualization of the morphology of the stationary phase. A Fourier-transform infrared (FTIR) system, CARY 630, Agilent Technologies (Santa Clara, USA), was used to provide the infrared spectra of monolith bulks, without any sample preparation. Evaluation of packing homogeneity in capillary columns was performed with scanning capacitively coupled contactless conductivity detection (sC<sup>4</sup>D). The C<sup>4</sup>D was a lab made system. A syringe pump was used to push

the capillary through the system with a constant speed ( $\text{cm s}^{-1}$ ).<sup>27,28</sup>

#### Chromatographic experiments

The chromatographic characterization was performed using an UltiMate 3000 capillary liquid chromatograph from Thermo Scientific (San Jose, USA). All the columns (20 cm × 100 μm i.d.) presented in Table 1 were evaluated, however, only columns A, B, C, D and H allowed the chromatographic characterization which requires permeability of the stationary phase. A test mixture containing six alkylbenzenes (benzene, toluene, ethylbenzene, propylbenzene, butylbenzene and pentylbenzene) and another with polycyclic aromatic hydrocarbons (PAH, naphthalene, anthracene, acenaphthene and pyrene) were dissolved in 70:30 (v/v) acetonitrile:water. The detection was performed at 215 and 254 nm using a UV-Vis detector from Thermo Scientific (San Jose, USA) with a detection cell of 3 nL, the injection volume was 35 nL. The separation was carried out at 25 °C with a flow rate of 1.2 μL min<sup>-1</sup> with a 45:55 (v/v) acetonitrile:water mobile phase. The data were processed using Chromeleon 6.8 software.



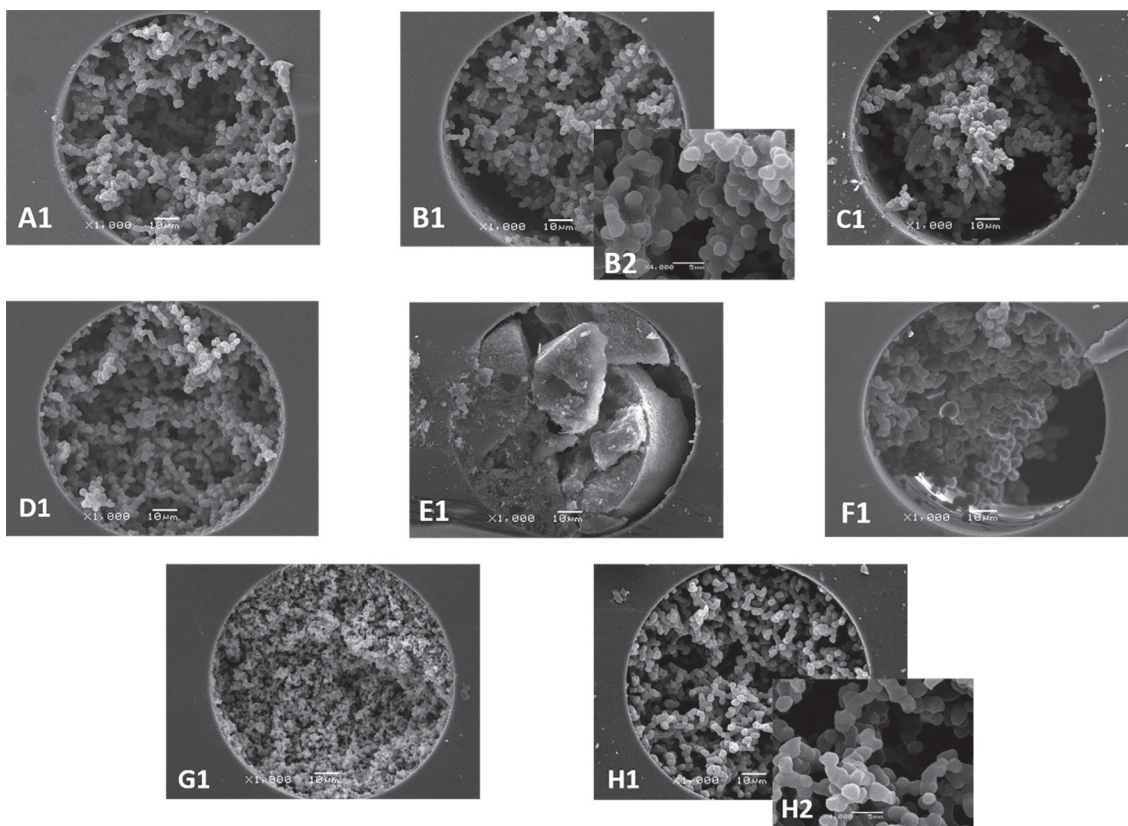


**Figure 1.** Scanning electron microscopy images of the hybrid columns (A-H) with 1000 $\times$  (1) and 4000 $\times$  (2) magnifications.

## Results and Discussion

### Physical characterization of the monolith

#### Scanning electron microscopy

The morphology of the synthesized monolithic materials A-H described in Table 1, can be seen in Figure 1. The SEM images show the effect of the contents of the mixtures on the structure of the monolithic material. Thus, monoliths with higher amounts of urea (E, F and G) presented a solid or very dense monolithic filling, due to thermal decomposition of urea at elevated temperatures.<sup>22</sup> Despite the good morphology of column B, the micrograph displays incomplete adhesion to the capillary tube wall, showing shrinkage of the material. Columns A, D and H present a structure with good adhesion to the inner wall of the capillary, small domains and no shrinkage.

#### Fourier-transform infrared (FTIR) spectroscopy

The infrared spectra of the bulks of monoliths 1-4 (Scheme 1), as shown in Figure 2, were measured to evaluate the surface derivatization of the monolithic materials. The absorption bands at 2924, 2855, 1621, 1457 and 1032  $\text{cm}^{-1}$  correspond to thiol alkane chain  $-\text{CH}_2$ .<sup>29-32</sup> Comparing spectra 3 and 4 of the monoliths, it is possible to see more

intense absorption bands at 778  $\text{cm}^{-1}$  of thiol due the higher content of vinyl groups<sup>31,33</sup> and the alkyl chain, represented by the two peaks in the region of 2924 and 2855  $\text{cm}^{-1}$  that show C-H stretching of methyl and methylene groups.<sup>30</sup> These results are in agreement with the literature.<sup>16,34,35</sup>

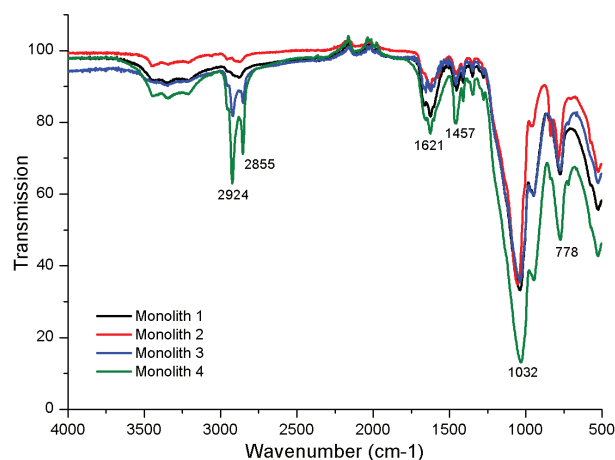


**Figure 2.** FTIR spectra from the different steps in the synthesis of the monolith matrix of column H.

#### Scanning capacitively coupled conductivity detection (sC<sup>4</sup>D)

In 2004, Connolly *et al.*<sup>27</sup> presented the first practical application of sC<sup>4</sup>D, using this technique to accurately

identify the location of tiny cracks in a silica monolith capillary column. A physical profiling of the monolithic columns is obtained when using this technique along with optical and electron microscopy. Analyzing Figure 3, a flat signal can be seen evidencing either a void column or a constant filling, plus a noise signal. This is feature of a heterogeneous filling, according to Connolly *et al.*<sup>27</sup> and Nesterenko *et al.*<sup>36</sup> A noiseless profile was also observed by Nesterenko *et al.*<sup>36</sup> in a monolithic porous layer open tubular (monoPLOT) capillary column. Column B presents

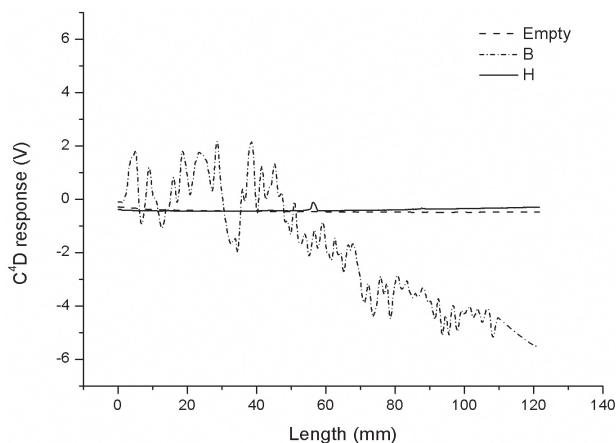


**Figure 3.** Scanning capacitively coupled contactless conductivity detection (sC<sup>4</sup>D) profiles of three different columns, an empty one (dashed line), column B (dash-dotted line), and column H (solid line).

a good morphology in SEM images but in sC<sup>4</sup>D it shows an unstable profile, higher density from the beginning to the middle of the column and a lower density from the middle to the end, resulting in a poorer column, compared to column H. On the other hand, column H exhibits a constant signal that, when evaluated together with the SEM image, characterizes a well-filled capillary. Other scans of the synthesized columns (A, C, D, E, F and G) can be found in Figure S1 (Supplementary Information (SI) section).

### Chromatographic evaluation

#### Chromatographic evaluation of the hybrid monolithic capillary columns

The vinyl-thiol-ene hybrid monolithic columns (monolith 4) were used for the separation of alkylbenzenes, shown in Figure 4. Columns E, F and G could not be tested chromatographically due to clogging of the columns. Columns A, C and D do not present good efficiency despite their homogeneous structure. Monolith C was not totally adhered to the column wall, probably the cause of lower efficiency. The higher permeability of column D (Table 1) can be explained by the low difference of backpressure between the filled and empty column, indicating holes in the structure and lower efficiency.<sup>29</sup> Column B showed good separation of the compounds, as did column H, and both

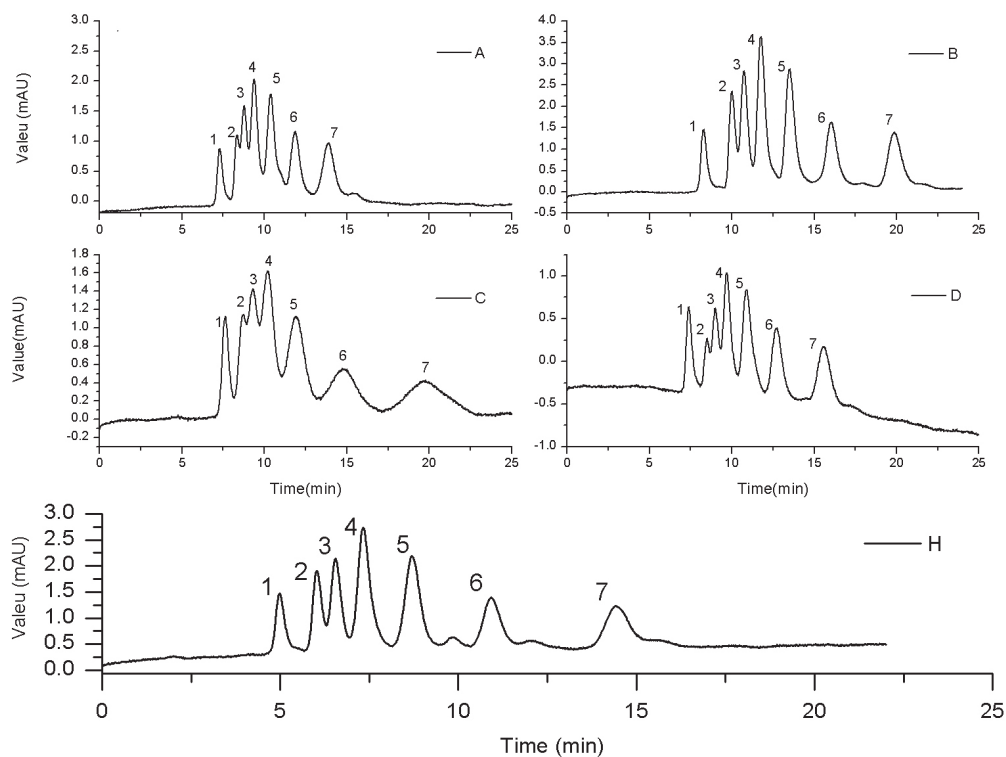


**Figure 4.** Separation of alkylbenzenes with vinyl-thiol-ene hybrid columns (A, B, C, D and H) using 50:50 (v/v) ACN:H<sub>2</sub>O, flow rate 0.7  $\mu\text{L min}^{-1}$ , detection 215 nm, 3 nL flow cell and 35 nL injections. Alkylbenzenes: (1) uracil; (2) benzene; (3) toluene; (4) ethylbenzene; (5) propylbenzene; (6) butylbenzene and (7) pentylbenzene.

present good efficiencies, asymmetries and resolutions, as can be seen in Table 1, which presents these chromatographic parameters. Based on the SEM images, chromatographic performance and analysis of the sC<sup>4</sup>D profiles, it can be concluded that column H presented the best results. This is due to a constant internal morphology along the capillary, as evidenced by the measured sC<sup>4</sup>D profile. Figure 5 shows the chromatograms for alkylbenzenes and PAH obtained with column H, leading to a satisfactory separation of these compounds. Capillary monolithic columns B and H presented efficiencies (plates m<sup>-1</sup>) of 15900 and 16500, respectively, with asymmetries (As<sub>10%</sub>) of 1.2 in both cases. Efficiency values above 20000 plates m<sup>-1</sup> for capillary monolithic columns are considered satisfactory for chromatographic separations,<sup>37</sup> although the literature presents values between 90000-110000 plates m<sup>-1</sup> for other types of hybrid monoliths.<sup>38-40</sup> For asymmetry, values between 0.9 and 1.2 are considered satisfactory according to the United States Pharmacopeia (USP).<sup>41</sup>

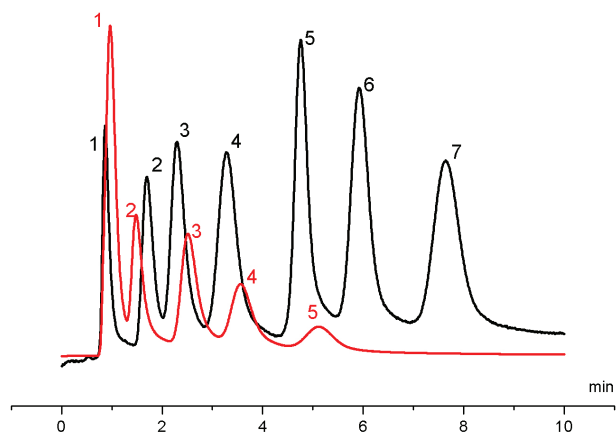


**Figure 5.** Chromatograms with column H. Separation of alkylbenzenes (black) and PAH (red) using ACN:H<sub>2</sub>O 50:50 (v/v), flow rate 2.0  $\mu\text{L min}^{-1}$ , detection 215 nm, 3 nL flow cell and 35 nL of injection. Alkylbenzenes (black): (1) uracil; (2) benzene; (3) toluene; (4) ethylbenzene; (5) propylbenzene; (6) butylbenzene and (7) pentylbenzene; PAH (red): (1) uracil; (2) naphthalene; (3) anthracene; (4) acenaphthene and (5) pyrene.

To compare the columns having monoliths 3 and 4, a mixture of alkylbenzenes was used, as seen in Figure 6. Monolith 3 does not present selectivity, which can be explained by the low presence of functional groups on the surface of the material.<sup>42</sup> The third step of the synthesis increases the content of vinyl groups in the matrix of monolith 4, allowing the separation of the proposed compounds with good efficiency.<sup>22</sup>

A bonded-phase with C<sub>12</sub> alkyl group (monolith 5) was prepared from monolith 1, filling the capillary with a solution of TCDDs in toluene, in different proportions. In this case, monolith 1 was used because of the presence

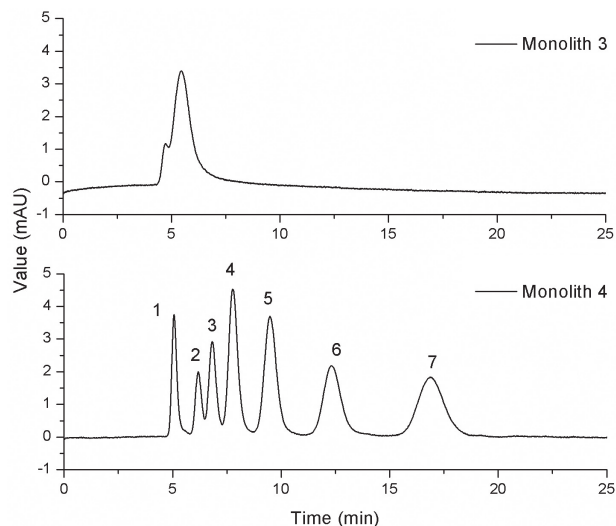


**Figure 6.** Comparison of the chromatographic profiles of monoliths 3 and 4. Separation of the alkylbenzene mixture using ACN:H<sub>2</sub>O 45:55 (v/v), flow rate 1.2  $\mu\text{L min}^{-1}$ , detection 215 nm, 3 nL flow cell and 35 nL injections. Identification of the compounds as in Figure 5.

of surface silanol groups, which are suitable for surface derivatization, while monolith 2 is rich in vinyl groups, incompatible with traditional alkylsilane reactions. The contents of TCDDs in the solutions, 30% (column I), 50% (column J) and 70% (column K), provided columns with different features. Columns I and J did not present clogging, had a homogeneous optical morphology and permeabilities of  $7.470 \times 10^{-14}$  and  $3.760 \times 10^{-14}$  m<sup>2</sup>, respectively, but lower efficiencies (1400 and 4300 plates m<sup>-1</sup>, respectively), compared to column H (16500 plates m<sup>-1</sup>), probably due to the lack of homogeneity of the groups on the surface of monolith 1. Column K, prepared using the 70% solution, got clogged and did not allow chromatographic evaluation. This can be explained by the high content of trichlorosilane groups causing a higher cross polymerization, leading to clogging. On the other hand, the hypervinylization reaction with VDMES on monolith 2 ensured that all the sites were replaced by vinyl groups, which were suitable for the thiol-ene reaction, resulting in a stable phase with good efficiency.

To compare the separation profiles of monoliths 4 and 5 (dodecanethiol and dodecanesilane), the chromatographic evaluations of columns H, I and J were performed using 45:55 (v/v) ACN:H<sub>2</sub>O, flow rate 1.2  $\mu\text{L min}^{-1}$ . As shown in Figure 7, the efficiency of columns I and J was still lower than that of the thiol-ene hybrid monolithic column (H).

#### Chemical stability

The column stability of the hybrid monolith synthesized with dodecanethiol was performed for 8000 column volumes (185 injections, one every 35 min) using the same chromatographic conditions as presented in Figure 5. As

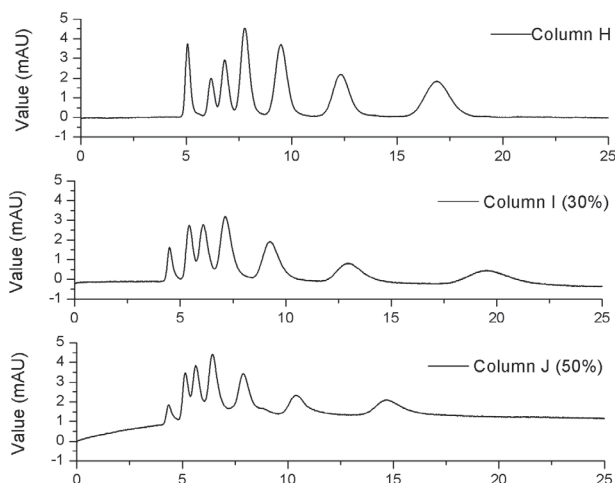


**Figure 7.** Effect of the volume ratio of dodecanesilane in toluene on the efficiency, comparing dodecanethiol columns and a dodecyl-functionalized hybrid silica column. Separation of the alkylbenzene mixture using ACN:H<sub>2</sub>O 45:55 (v/v), flow rate 1.2  $\mu\text{L min}^{-1}$ , detection 215 nm, 3 nL flow cell and 35 nL of injection.

seen in Figure 8, the asymmetry and retention factor were unchanged throughout the chromatographic analyses of uracil and propylbenzene up to the end of the test. The stability presented for this dodecanethiol hybrid monolithic column are probably due to the fact that the cleavage of the Si–S bond on the surface silica is difficult to occur. This kind of test, despite being important, is not commonly reported in monolithic column evaluations.

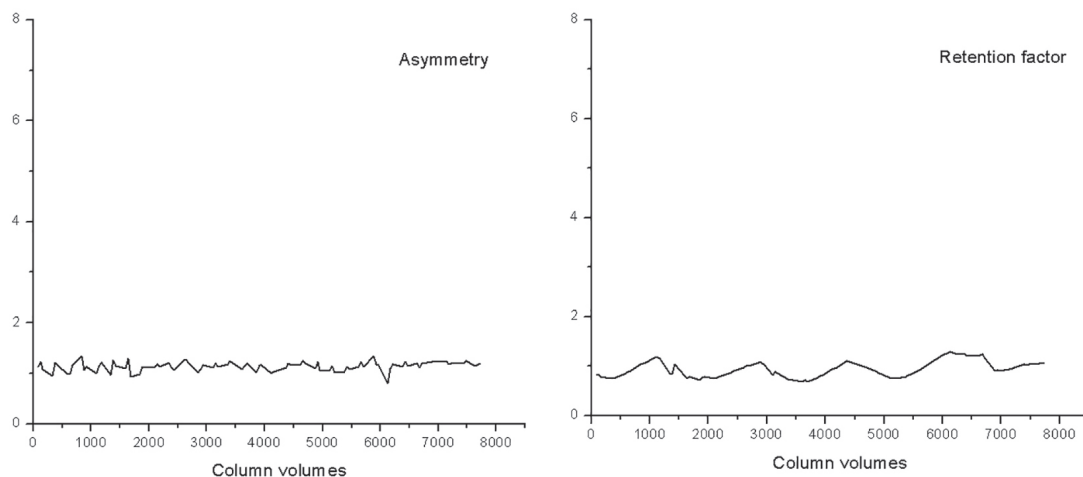


**Figure 8.** Chemical stability of dodecanethiol stationary phase (column H) for 8000 column volumes. The chromatographic conditions were ACN:H<sub>2</sub>O 45:55 (v/v); 1.2  $\mu\text{L min}^{-1}$ , detection 215 nm, 3 nL flow cell and 35 nL injections. The compounds used for the evaluations were uracil and propylbenzene in both cases.

## References

- Silva, R. G. C.; Collins, C. H.; Bottoli, C. B. G.; *Quim. Nova* **2011**, *34*, 841.
- Racha, E.-D.; Gay, P.; Dugas, V.; Demesmay, C.; *J. Sep. Sci.* **2016**, *39*, 842.

## Conclusions

A vinyl-functionalized polymer-silica hybrid monolith was successfully prepared through the sol-gel process followed by derivatization via thiol-ene click chemistry. The optimized dodecanethiol monolithic column showed a homogeneous morphology without shrinkage, reasonable efficiency (around 16000 plates  $\text{m}^{-1}$ ), and chemical stability to at least 8000 column volumes. Compared to a dodecanesilane bonded phase, the vinyl thiol-ene hybrid columns exhibited higher efficiency and satisfactory separation performance.

## Supplementary Information

Supplementary data are available free of charge at <http://jbcbs.sbg.org.br> as PDF file.

## Acknowledgments

The authors acknowledge financial support from the Fundação de Amparo à Pesquisa do Estado de São Paulo (FAPESP), grant 2014/50867-3 and the Conselho Nacional de Desenvolvimento Científico e Tecnológico (CNPq), grants 311671/2015-2 and 465389/2014-7. This work was supported by the National Institute of Bioanalytical Chemistry (INCT Bioanalítica). The authors also thank Professor Carol H. Collins for language assistance.

- Zajickova, Z.; *J. Sep. Sci.* **2017**, *40*, 25.
- Núñez, O.; Nakanishi, K.; Tanaka, N.; *J. Chromatogr. A* **2008**, *1191*, 231.
- Jandera, P.; Urban, J.; Škeříková, V.; Langmaier, P.; Kubíčková, R.; Planeta, J.; *J. Chromatogr. A* **2010**, *1217*, 22.
- Nazario, C. E. D.; Silva, M. R.; Franco, M. S.; Lanças, F. M.;



- J. Chromatogr. A* **2015**, *1421*, 18.
7. Wu, R.; Hu, L.; Wang, F.; Ye, M.; Zou, H.; *J. Chromatogr. A* **2008**, *1184*, 369.
  8. Hong, T.; Yang, X.; Xu, Y.; Ji, Y.; *Anal. Chim. Acta* **2016**, *931*, 1.
  9. Tanaka, N.; Unger, K. K. In *Monolithic Silicas in Separation Science - Concepts, Syntheses, Characterization, Modeling and Applications*; Unger, K. K.; Tanaka, N.; Machtejevas, E., eds.; Wiley-VCH: Weinheim, 2011, p. 2-4.
  10. Liu, S.; Peng, J.; Liu, Z.; Liu, Z.; Zhang, H.; Wu, R.; *Sci. Rep.* **2016**, *6*, 34718.
  11. Guiochon, G.; *J. Chromatogr. A* **2007**, *1168*, 101.
  12. Ou, J.; Liu, Z.; Wang, H.; Lin, H.; Dong, J.; Zou, H.; *Electrophoresis* **2015**, *36*, 62.
  13. Hayes, J. D.; Malik, A.; *Anal. Chem.* **2000**, *72*, 4090.
  14. Wu, M.; Wu, R.; Zhang, Z.; Zou, H.; *Electrophoresis* **2011**, *32*, 105.
  15. Zhang, Z.; Hao, Y. H.; Ding, J.; Xu, S. N.; Yuan, B. F.; Feng, Y. Q.; *J. Chromatogr. A* **2015**, *1416*, 64.
  16. Liu, Z.; Liu, J.; Liu, Z.; Wang, H.; Ou, J.; Ye, M.; Zou, H.; *J. Chromatogr. A* **2017**, *1498*, 29.
  17. Zhang, Z.; Lin, H.; Ou, J.; Qin, H.; Wu, R.; Dong, J.; Zou, H.; *J. Chromatogr. A* **2012**, *1228*, 263.
  18. Ou, J.; Lin, H.; Zhang, Z.; Huang, G.; Dong, J.; Zou, H.; *Electrophoresis* **2013**, *34*, 126.
  19. Jonnada, M.; Rathnasekara, R.; El Rassi, Z.; *Electrophoresis* **2015**, *36*, 76.
  20. Liu, Z.; Ou, J.; Zou, H.; *TrAC, Trends Anal. Chem.* **2016**, *82*, 89.
  21. Kolb, H. C.; Finn, M. G.; Sharpless, K. B.; *Angew. Chem., Int. Ed.* **2001**, *40*, 2004.
  22. Wang, K.; Chen, Y.; Yang, H.; Li, Y.; Nie, L.; Yao, S.; *Talanta* **2012**, *91*, 52.
  23. Lv, X.; Tan, W.; Chen, Y.; Chen, Y.; Ma, M.; Chen, B.; Yao, S.; *J. Chromatogr. A* **2016**, *1454*, 49.
  24. Wang, H.; Hu, W.; Zheng, Q.; Bian, W.; Lin, Z.; *J. Sep. Sci.* **2017**, *40*, 2344.
  25. Zeng, J.; Liu, S.; Wang, M.; Yao, S.; Chen, Y.; *Electrophoresis* **2017**, *38*, 1325.
  26. Bristow, P. A.; Knox, J. H.; *Chromatographia* **1977**, *10*, 279.
  27. Connolly, D.; Floris, P.; Paull, B.; Nesterenko, P. N.; *TrAC, Trends Anal. Chem.* **2010**, *29*, 870.
  28. Brito-Neto, J. G. A.; da Silva, J. A. F.; Blanes, L.; do Lago, C. L.; *Electroanalysis* **2005**, *17*, 1198.
  29. Ma, S.; Zhang, H.; Li, Y.; Li, Y.; Zhang, N.; Ou, J.; Ye, M.; Wei, Y.; *J. Chromatogr. A* **2018**, *1538*, 8.
  30. Zhang, N.; Zhang, L.; Qiao, X.; Wang, Y.; Yan, H.; Bai, L.; *RSC Adv.* **2015**, *5*, 91436.
  31. Shen, S.; Ye, F.; Zhang, C.; Xiong, Y.; Su, L.; Zhao, S.; *Analyst* **2014**, *140*, 265.
  32. Liu, Z.; Ou, J.; Lin, H.; Wang, H.; Dong, J.; Zou, H.; *J. Chromatogr. A* **2014**, *1342*, 70.
  33. Lin-Vien, D.; Colthup, N. B.; Fateley, W. G.; Grasselli, J. G.; *The Handbook of Infrared and Raman Characteristic Frequencies of Organic Molecules*, vol. 4; Elsevier: San Diego, 1991, p. 225-250.
  34. Alimohammadi, F.; Wang, C.; Durham, O. Z.; Norton, H. R.; Bowman, C. N.; Shipp, D. A.; *Polymer (Guildf.)* **2016**, *105*, 180.
  35. Liu, Z.; Ou, J.; Lin, H.; Wang, H.; Liu, Z.; Dong, J.; Zou, H.; *Anal. Chem.* **2014**, *86*, 12334.
  36. Nesterenko, E. P.; Burke, M.; de Bosset, C.; Pessutto, P.; Malafosse, C.; Collins, D. A.; *RSC Adv.* **2015**, *5*, 7890.
  37. da Silva, C. G. A.; Collins, C. H.; Bottoli, C. B. G.; *Microchem. J.* **2014**, *116*, 249.
  38. Codesido, S.; Rudaz, S.; Veuthey, J.-L.; Guilleme, D.; Desmet, G.; Fekete, S.; *J. Chromatogr. A* **2019**, *1603*, 208.
  39. Chen, M. L.; Zhang, J.; Zhang, Z.; Yuan, B. F.; Yu, Q. W.; Feng, Y. Q.; *J. Chromatogr. A* **2013**, *1284*, 118.
  40. Lin, H.; Ou, J.; Zhang, Z.; Dong, J.; Wu, M.; Zou, H.; *Anal. Chem.* **2012**, *84*, 2721.
  41. Snyder, L. R.; Kirkland, J. J.; Dolan, J. W.; *Introduction to Modern Liquid Chromatography*, 3<sup>rd</sup> ed.; Wiley: Hoboken, USA, 2010.
  42. Kirkland, J. J.; Glajch, J. L.; Farlee, R. D.; *Anal. Chem.* **1989**, *61*, 2.

Submitted: February 8, 2019

Published online: July 26, 2019

